The Genomes of Nematode-Trapping Fungi Provide Insights into the Origin and Diversification of Fungal Carnivorism

Yani Fan[1,3,8], Minghao Du[2,8], Weiwei Zhang[1,3,8], Wei Deng[4,8], Ence Yang[2], Shunxian Wang[4], Luwen Yan[4], Liao Zhang[4], Seogchan Kang[5], Jacob L Steenwyk[6], Zhiqiang An[7], Xingzhong Liu[4,*], and Meichun Xiang[1,3,*]

[1] State Key Laboratory of Mycology, Institute of Microbiology, Chinese Academy of Sciences, Beijing 100101, China.

[2] Department of Microbiology, School of Basic Medical Sciences, Peking University Health Science Center, Beijing 100191, China.

[3] University of Chinese Academy of Sciences, Beijing 100049, China.

[4] State Key Laboratory of Medicinal Chemical Biology, Key Laboratory of Molecular Microbiology and Technology of the Ministry of Education, Department of Microbiology, College of Life Science, Nankai University, Tianjin 300071, China.

[5] Department of Plant Pathology & Environmental Microbiology, Pennsylvania State University, PA 16802, USA.

[6] Howards Hughes Medical Institute and Department of Molecular and Cell Biology, University of California, Berkeley, CA 94720, USA

[7] Texas Therapeutics Institute, The Brown Foundation Institute of Molecular Medicine, University of Texas Health Science Center, Houston, TX 77030, USA.

[8] These authors contributed equally.

*Correspondence authors: Xingzhong Liu (liuxz@nankai.edu.cn) and Meichun Xiang (xiangmc@im.ac.cn).

Abstract

Nematode-trapping fungi (NTF), most of which belong to a monophyletic lineage in Ascomycota, cannibalize nematodes and other microscopic animals, raising questions regarding the types and mechanisms of genomic changes that enabled carnivorism and adaptation to the carbon-rich and nitrogen-poor environment created by the Permian-Triassic extinction event. Here, we conducted comparative genomic analyses of 21 NTF and 21 non-NTF to address these questions. Carnivorism-associated changes include expanded genes for nematode capture, infection, and consumption (e.g., adhesive proteins, CAP superfamily, eukaryotic aspartyl proteases, and serine-type peptidases). Although the link between secondary metabolite (SM) production and carnivorism remains unclear, we found that the numbers of SM gene clusters among NTF are significantly lower than those among non-NTF. Significantly expanded cellulose degradation gene families (GH5, GH7, AA9, and CBM1) and contracted genes for carbon-nitrogen hydrolases (enzymes that degrade organic nitrogen to ammonia) are likely associated with adaptation to the carbon-rich and nitrogen-poor environment. Through horizontal gene transfer events from bacteria, NTF acquired the *Mur* gene cluster (participating in synthesizing peptidoglycan of the bacterial cell wall) and *Hyl* (a virulence factor in animals). Disruption of *MurE* reduced NTF's ability to attract nematodes, supporting its role in carnivorism. This study provides new insights into how NTF evolved and diversified after the Permian-Triassic mass extinction event.

Introduction

Fungi employ diverse strategies to acquire nutrients for growth and reproduction. Carnivorous nematode-trapping fungi (NTF) develop sophisticated trapping devices to capture and consume nematodes and other microscopic animals, such as amoebas, rotifers, and springtails (Pramer 1964). Although carnivorous fungi have been found in multiple phyla, more than 90% of the known NTF belong to the class Orbiliomycetes, a monophyletic lineage in Ascomycota (Yang et al. 2007). Ascomycota NTF develop adhesive traps and constricting rings to capture and consume nematodes, the most abundant soil animals (Nordbringhertz and Stalhammarcarlemalm 1978; van den Hoogen et al. 2019). The rarity of carnivorism among fungi has raised great interest in unraveling the origin and evolution of carnivorous traits.

The evolution of carnivorous Orbiliomycetes has been studied using multilocus phylogenetic analysis (Li et al. 2005; Yang et al. 2007; Yang et al. 2012). According to molecular clock estimates, fungi employing active carnivorism (forming constricting rings) and those engaging in passive carnivorism (forming adhesive traps) diverged shortly after the Permian-Triassic mass extinction event (Yang et al. 2012). This event resulted in a marked increase of dead plant material (Visscher et al. 1996), creating carbon rich and nitrogen poor environment. Barron (2003) hypothesized that NTF evolved the ability to capture nematodes to supplement nitrogen. Several NTF traits support this hypothesis. First, trap morphogenesis is induced only when free-living nematodes are present and usually requires physical contact between hyphae and nematodes (Tunlid et al. 1992; de Ulzurrun and Hsueh 2018). Second, NTF actively attract nematodes to their mycelia and hold them during trap formation (Lopez-Llorca et al. 2007; de Ulzurrun and Hsueh 2018). In addition, NTF's high lignolytic and cellulolytic activities, which are advantageous for living in carbon-rich environments, have been well documented (Barron 1992; Barron 2003).

Comparative and evolutionary genomics has shed light on niche adaptation and the evolution of the genotype-phenotype map across the map (Watkinson 2016; Steenwyk and Rokas 2017; Murat et al. 2018; Steenwyk et al. 2019; Smith et al. 2020; Bajic and Sanchez 2020; Malar et al. 2021). For example, evolutionary dynamics of carbon and nitrogen metabolism have been illuminated from comparative genomics of Saccharomycotina yeast (Opulente et al. 2023). Similarly, the ancient origin of woody plant material degradation (i.e., lignin degradation) in mushroom forming fungi has

also been charted using comparative evolutionary genomics (Floudas et al. 2012). Accordingly, comparative genome analyses between NTF and non-NTF hold promise to uncover candidate genomic changes underlying the evolution of nematode trapping capabilities.

Here, we conducted comparative and phylogenomic analyses of 21 NTF and 21 non-NTF Ascomycota species and identified candidate carnivorism-associated genomic changes, including horizontally transferred bacterial genes, and genomic adaptation to carbon-rich/nitrogen-poor environments. One of the horizontally transferred genes was disrupted, revealing an involvement in carnivorism. Transcriptome analysis of three NTF (*Drechslerella dactyloides*, *Dactylellina haptotyla* and *Arthrobotrys oligospora*) in the absence and presence of the nematode *Caenorhabditis elegans* (Fan et al. 2021; Yang et al. 2022) revealed that some candidate carnivorism-associated genes, like adhesive protein-coding genes, were up-regulated in the presence of nematodes. Together, these analyses reveal multiple dimensions of genomic changes that contributed to the evolutionary trajectory of NTF.

Results

Characteristics of the NTF genomes

The NTF genomes analyzed (16 *de novo* sequenced and 5 downloaded from GenBank) included 4 *Drechslerella* spp. forming mechanical constricting rings, 9 *Arthrobotrys* spp. forming 3-dimensional (3-D) adhesive nets, 8 *Dactylellina* spp. forming 2-D traps with the exception of *Da. cionopaga* (forming adhesive columns), and 7 other species forming adhesive knobs (Supplementary Table 1). Genome sizes ranged from 30.2 to 54.2 Mb (median 39.0 Mb), with the number of predicted protein-coding genes varying from 7,955 to 13,112 (Table 1) and 60.9-70.0% of the genes being annotated to encode proteins with Pfam domain(s). Although the N50 values of the *Da. entomopaga* (579 Kb), *Da. haptotyla* (177 Kb) and *Da. drechsleri* (743 Kb) genomes were much lower than those of the other NTF genomes (1.2-6.2 Mb), examination of near-universally single-copy orthologs (or BUSCO genes) indicated high gene content completeness (93.7-96.1%).

We compared the 21 NTF genomes with the genomes of 21 non-NTF species (Ascomycota) representing diverse lifestyles, including saprophytic, mutualistic, phytopathogenic, endophytic, entomopathogenic, and nematode endoparasitic (Fig.

1A; Supplementary Tables 1 and 2). We identified 22,679 orthologous groups (OGs) among the 458,922 protein-coding genes on the 42 genomes using OrthoFinder (Supplementary Table 3). Species-specific OGs account for 0-6.3%, and 25.1-47.2% of the OGs in each species are present in all 42 genomes (Fig. 1B; Supplementary Table 4). In total, 514 OGs are NTF-specific and present in all NTF, accounting for 5.4-6.8% of the total genes in each species (Fig. 1B; Supplementary Table 5). However, 65.4% of the NTF-specific OGs could not be annotated (orphan genes). Some OGs are unique to each NTF lineage and may be associated with unique trapping strategies: 52 OGs in 3-D adhesive net-forming species, 16 OGs in 2-D adhesive net-forming species, and 31 OGs in mechanical trap-forming species.

Functional enrichment analysis of the NTF-specific OGs containing Pfam domain(s) showed significant enrichment of multiple gene families related to nematode capture (CFEM domain and putative adhesin) and infection and digestion [cysteine-rich secretory protein family (CAP superfamily), eukaryotic aspartyl protease (ASP), and subtilase family]. In addition, cellulose-binding domains (fungal cellulose-binding domain and WSC domains), protein ubiquitination degradation-related domains (F-box domain, ubiquitin-conjugating enzyme), amino acid permeases, and Mur proteins (involved in synthesizing peptidoglycan, a main component of the bacterial cell wall) are significantly enriched in the NTF-specific OGs (Fig. 1C; Supplementary Table 7). A search of the Non-Redundant Protein Sequence Database using the 514 NTF-specific OGs and subsequent HGTector analysis revealed 89 putative horizontal gene transfer (HGT) events. Four OGs containing different Mur protein domains and one OG with a “polysaccharide lyase family 8 domain” may participate in carnivorism. These domains exhibit significant sequence similarity to bacterial proteins but lack homologous fungal proteins (Supplementary Table 8), suggesting their horizontal gene transfer (HGT) from bacteria.

Principal component analysis (PCA) revealed significant differences in the conserved Pfam domains between NTF and non-NTF. NTF formed a discrete cluster separated from non-NTF according to PC1 (Fig. 2A). The Pfam domains that contributed the most (top 10%, 451 Pfam domains) to PC1 included 153 expanded and 298 contracted domains (Fig. 2B; Supplementary Table 9). The expanded genes include (a) those encoding extracellular proteins such as “Egh16-like virulence factor”, and “cysteine-rich secretory protein family”, (b) proteases such as “Matrixin”, protein ubiquitination degradation-related domains such as “F box”, and (c) cellulose-binding modules such

as “fungal cellulose-binding domain”. In contrast, the genes for carbon-nitrogen hydrolases and secondary metabolism, such as “cytochrome P450”, “polyketide synthase dehydratase”, and “acyl transferase domain”, were contracted (Supplementary Table 9).

Genome changes likely associated with adaptation to carbon-rich and nitrogen-poor environments

The hypothesis that fungal carnivorism evolved in response to mass extinction was proposed (Barron 2003) but has not been tested (Yang et al. 2012). Analysis of the gene families involved in carbohydrate metabolism (Supplementary Table 10) showed that the number of carbohydrate-active enzyme (CAZyme) genes ranged from 278 to 500 in NTF (mean of 409), which is significantly lower than that in plant-associated non-NTF (endophytic: mean of 786, $p = 0.0252$; phytopathogenic: mean of 591, $p = 0.0007$; mutualistic: mean of 570, $P = 0.0085$) but significantly higher than that in animal parasitic non-NTF, such as entomopathogenic (mean of 352, $p = 0.0027$) and nematode-endoparasitic fungi (mean of 269, $p = 0.0333$) (Fig. 3A). Moderate expansion of the genes encoding cellulose-degrading enzymes, including GH5, GH7, and AA9, in NTF likely enhanced their cellulose-degrading capability. Moreover, the NTF genomes encode a larger set of proteins carrying one or more carbohydrate-binding modules (CBM) compared to the non-NTF genomes (Fig. 3B). CBMs, particularly CBM1 (Chundawat et al. 2021), are essential for cellulases to bind to the cellulose surface, thus enhancing the efficiency of cellulose-degrading enzymes (Espagne et al. 2008; Klosterman et al. 2011; Liu et al. 2014). The number of cellulose-degrading enzymes with CBM1 in NTF is much higher than that in non-NTF (Mann-Whitney U test) (Fig. 3C; Supplementary Table 11), a feature that likely enhanced NTF’s ability to degrade cellulose.

Carnivorous fungi prey on nematodes to supplement nitrogen intake (Barron 2003; Yang et al. 2012; Lee et al. 2020). The gene family encoding carbon-nitrogen hydrolases (EC 3.5.1.-) contracted in NTF (Fig. S1; Supplementary Table 12). These hydrolases conserved among NTF (Fig. S1) belong to the nitrilase superfamily, which can break carbon-nitrogen bonds to degrade organic nitrogen compounds and produce ammonia (Pace and Brenner 2001). In contrast, many more carbon-nitrogen hydrolase coding genes were identified in entomopathogens and nematode endoparasites, suggesting that they mainly utilize protein-derived nutrients for energy (Supplementary Table 12). The genes encoding amino acid permeases are enriched in

the NTF-specific OGs and contribute to amino acid transport (Supplementary Tables 7). These patterns suggest that NTF evolved to utilize organic nitrogen more efficiently by contracting carbon-nitrogen hydrolase genes (to reduce the loss of nitrogen in the form of ammonia) and gaining specific amino acid permease genes (to assimilate nitrogen in nitrogen-poor environments), supporting the hypothesis that these genomic changes were selected to help NTF adapt to nitrogen-poor conditions.

Genome evolution putatively linked to carnivorism

NTF are expected to secrete numerous proteins that participate in capturing and consuming nematodes. We compared the predicted secreted proteins between NTF and non-NTF. The number of secreted proteins ranged from 284 to 1,654 (Fig. S2; Supplementary Tables 12 and 13). After normalization using the total number of genes for each genome, the ratio of secreted proteins encoded by NTF was significantly higher than that of non-NTF (p-value < 0.0001, Mann-Whitney U test), suggesting ancestral burst of the secreted protein repertoire.

The extracellular adhesive layer of traps is essential for nematode capture. Three types of adhesive proteins, including those containing GLEYA (PF10528), Egh16-like (PF11327), and CFEM (PF05730), were predicted to be involved in capturing nematodes (Liang et al. 2015; Ji et al. 2020; Zhang et al. 2020). These adhesive proteins accounted for more than 2% of the secreted proteins in all NTF, which is higher than that in non-NTF (Fig. 4A; Supplementary Table 14). In addition, the ratios of GLEYA domains (p-value =< 0.0001, Mann-Whitney U test) and Egh16-like domains (p-value < 0.0001, Mann-Whitney U test) in NTF are significantly higher than those in non-NTF. Gene expression patterns in three representative NTF (*Ar. oligospora*, *Da. haptotyla* and *Dr. dactyloides*) during nematode capture showed that the genes for 9.5% (2/21) of the adhesive proteins with a GLEYA domain and 15.2% (5/33) of the adhesive proteins with an Egh16-like domain were up-regulated (Supplementary Tables 15 and 17), supporting the hypothesis that expansion and up-regulation of adhesive protein-coding genes represent a genomic adaptation for a predatory lifestyle.

The nematode cuticle is a three-layered structure consisting mainly of collagen and noncollagenous proteins. The CAP superfamily (PF00188), composed of cysteine-rich secretory proteins, antigen 5, and pathogenesis-related 1 proteins, expanded among NTF (Supplementary Table 9). This superfamily participates in reproduction,

213 virulence, venom toxicity, cellular defense, and immune evasion (Gibbs et al. 2008;
214 Darwiche et al. 2016). All three NTF analyzed showed that 36.4% (4/11) of the CAP
215 superfamily genes were up-regulated in the presence nematodes (Supplementary
216 Tables 15 and 18), suggesting their involvement in nematode infection. In addition,
217 the genes for serine peptidases, which are involved in nematode consumption, also
218 significantly expanded in NTF (Fig. 4B), and 15.6% (10/64) of the genes encoding
219 members of the subtilisin family in three NTF were up-regulated during predation
220 (Supplementary Tables 15 and 19).

221 Fungi produce diverse secondary metabolites (SMs), some of which are “chemical
222 weapons” against other organisms (Rohlfs and Churchill, 2011; Keller 2019).
223 Significantly reduced numbers of and less conserved SM gene clusters among NTF
224 suggest that broad capacity for SMs production is not critical for carnivorism.
225 However, similar to other Ascomycota fungi, individual SMs may be important for
226 organismal ecology (Raffa and Keller, 2019; Steenwyk et al. 2020a). The number of
227 predicted SM gene clusters ranged from 6 to 23 in NTF (mean of 13.14), which is
228 significantly lower than those of non-NTF: endophytic and phytopathogenic fungi
229 (mean of 49.42, $p < 0.0001$) and entomopathogenic and nematode-endoparasitic fungi
230 (mean of 59.29, $p < 0.0001$) (Fig. 4C; Supplementary Table 20). Only *T.*
231 *melanosporum*, a mutualistic ectomycorrhizal fungus, has 9 clusters. The PKS gene
232 clusters were not conserved among NTF, suggesting that this class of SMs may not be
233 critical for carnivorism and perform species-specific roles.

234 Non-vertical evolution, including HGT, has been instrumental in driving the rapid
235 adaptive evolution of fungi and has played a role in the emergence of new pathogens
236 (Feurtey and Stukenbrock, 2018; Steenwyk et al. 2020b). Among the 89 potential
237 HGT events observed in NTF, the HGT of *Mur* genes, which are involved in bacterial
238 cell wall biosynthesis (Radkov et al. 2018), is notable. Top 100 blastp results using *Ar.*
239 *oligospora* proteins revealed that 4 proteins with Mur domains were highly similar to
240 MurA (53.1-69.2% identity; 90-96% coverage), MurC (65.8-72% identity; 98–99%
241 coverage), MurD (63.7-70.2% identity; 98–99% coverage), and MurE (39.2-49.4%
242 identity; 92–98% coverage), respectively. Maximum-likelihood phylogenetic trees
243 were constructed using RAxML (Fig 5A, Fig. S3). The *MurE* gene was found in all
244 NTF, suggesting its horizontal transfer before NTF diversification. The presence of
245 introns in the NTF *MurE* gene indicates that the gene underwent eukaryotization. The
246 function of NTF *MurE* in carnivorism was studied by disrupting the gene in *Dr.*

dactyloides. Compared with the wild type, three independently isolated mutants showed reduced ability to attract *C. elegans* (p-value = 1.1e-4 , 2.5e-3 , 5.2e-4, two-tailed t-test, n = 5), with the attraction indices of the mutants being only 36.0% of that of the wild type (Fig. 5B).

Analysis using CLEAN (contrastive learning-enabled enzyme annotation), which predicts enzyme function (Gregoire et al. 2023), showed that one NTF-specific OG with the polysaccharide lyase family 8 domain is closely related to Hyl, a bacterial hyaluronate lyase (EC:4.2.2.1). Bacterial Hyl is an important virulence factor employed by Gram-positive bacteria to enhance their infectivity by degrading extracellular hyaluronate and chondroitin sulfate of animal hosts (Patil et al. 2023). All NTF species encode two Hyl homologs, except for *Dr. stenobrocha* (one homolog). The maximum-likelihood phylogenetic tree of this OG showed that the two homologs belong to distinct clades (Fig. S4), suggesting that they may have originated from different bacteria through two separate HGT events. Bacterial hyaluronate lyases are typically secreted; however, their NTF homologs lack a signal peptide. Most of one Hy1 clade have putative transmembrane domains, whereas those in the other clade lack transmembrane domains (Fig. S4). Further studies are required to determine whether Hyl homologs contribute to nematode carnivorism.

Discussion

Approximately 5 million years after the Permian-Triassic mass extinction event, the global ecosystem had stabilized and undergone extensive remodeling during the process (Ezcurra and Butler 2018; Rampino et al. 2020). The sharp increase in the biomass and diversity of taxa, including fungi, algae, and ferns, in the immediate aftermath of the plant collapse in the late Permian (Mays et al. 2020) indicated biotic recovery. The availability of new niches resulting from this mass extinction event likely accelerated innovation during recovery (Lowery and Fraass 2019).

The lifestyle of the fungi that gave rise to NTF after mass extinction remains unclear. In this study, we identified multiple genome changes—gene family gain/loss and HGT—that are associated with the evolution of NTF ecology and carnivorous lifestyle. For example, gene families that have been reported to play critical roles in trap morphogenesis (Yang et al. 2018; Yang et al. 2020; Zhang et al. 2021), such as components of the G-protein mediated signaling and ubiquitin-conjugating enzyme

Ubr1 (Supplementary Table 9), have expanded. Similarly, the genes of cell-surface proteins containing the carbohydrate-binding WSC domain were up-regulated during nematode infection (Andersson et al. 2013; 2014) and were found to be significantly expanded in NTF (Supplementary Table 9). Other expanded gene families that may be linked to fungal carnivorism are those encoding adhesive proteins and proteases such as subtilase (Liang et al. 2015; Wang et al. 2015; Ji et al. 2020; Zhang et al. 2020). Overall, the patterns of gene family expansion in NTF resemble those observed in plant pathogens rather than patterns found in insect and animal pathogens (Meerupati et al. 2013).

The evolution of various trapping devices by fungi to capture nematodes as a nitrogen source was hypothesized to be an innovation crucial for NTF (Yang et al. 2012). Here we found two changes that helped optimize this mode of nitrogen acquisition. Carbon-nitrogen hydrolase genes were reduced among NTF, a change critical for efficient utilization of nitrogen resources by reducing the decomposition of organic nitrogen compounds to ammonia. Meanwhile, genes for specific amino acid permeases expanded in NTF. Some class III aminotransferase genes, which help enhance nitrogen assimilation, are up-regulated during nematode capturing (Supplementary Table 16). These patterns suggest that NTF evolved to recycle nitrogen resources efficiently by remodeling their nitrogen metabolism.

Perhaps the most strikingly, NTF have horizontally acquired multiple *Mur* genes, which are involved in bacterial cell wall peptidoglycan synthesis, from bacteria to ensnare nematodes. Disruption of the *MurE* gene indicated its involvement in attracting nematodes (Fig. 5B). Phylogenetic analysis revealed that the constituents of the *Mur* gene cluster were acquired through multiple complex HGT events (Figs. 5A and S3). Gene clusters originating from multiple HGT events have been observed in *Saccharomycotina* yeast (Gonçalves C and Gonçalves P, 2019), and our analyses suggest this may be a more widespread phenomenon in fungi. The cell wall of the nematode traps seemed different from that of hyphae (Fig. S5), suggesting that cell wall composition may play a role in trapping nematodes. How the *MurE* gene contributes to nematode attraction and whether other *Mur* genes have similar roles remain to be investigated. However, their involvement in bacterial cell wall formation raises the possibility of their involvement in modifying fungal cell wall to attract nematodes.

Our study uncovered multiple modes of genomic changes that likely influenced the

evolutionary trajectory of NTF, implicating several gene families that have previously been shown to be linked to the NTF lifestyle. More importantly, our comprehensive analysis identified novel candidate genes and evolutionary processes that may underlie specific stages of predation—such as attraction and consumption. Taken together, our work established an extensive genome resource and ample hypotheses that will guide future studies to understand the origins and evolution of NTF and confirm the involvement of candidate genes associated with NTF lifestyles.

Materials and Methods

Strains, media, and culturing conditions

The NTF sequenced (Supplementary Table 1) were cultured on potato dextrose agar (PDA) and corn meal agar (CMA). Mycelia used for genomic DNA extraction were prepared by inoculating approximately 10^5 spores or ten 5-mm diameter plugs from freshly grown culture on PDA into 100 mL potato dextrose broth (PDB). After shaking the cultures at 120 rpm and 28 °C for 10 days, mycelia were collected using a glass cotton filter and washed three times with distilled water.

Whole-genome sequencing

Genomic DNA was extracted using a CTAB/SDS/Proteinase K method (Möller et al. 1992). Four genomic DNA libraries with insert sizes of 400 bp, 500 bp, 3 Kb, and 5-8 Kb, respectively were prepared. The library with 400 bp inserts was sequenced using Illumina PE250. The remaining libraries were sequenced using Illumina PE150. The resulting sequence reads were processed using Trimmomatic v0.38 to remove adapters and low-quality reads (Bolger et al. 2014). Processed reads were assembled de novo using ALLPATH-LG release 52488 (Gnerre et al. 2011). To improve completeness, draft assembled genomes were scaffolded using data from mate-pair libraries (3 Kb and 5-8 Kb) via two rounds of SSPACE-standard v3.0 (Boetzer et al. 2011). The output was used for the analyses described below. The completeness of individual genome assemblies and gene prediction was evaluated using BUSCO v4.0.2, based on Ascomycota ortholog database containing 1,706 orthologs (Boetzer et al. 2011).

Gene prediction and functional annotation

Regions of repetitive sequence elements in the assembly were masked using RepeatMasker v4.0.7 based on a species-specific repeat library generated using RepeatModeler v4.0.7. For structural annotation, the quality of protein sequence predictions was assessed via BUSCO analysis. The BRAKER pipeline (Hoff et al. 2016) was used to test protein homology. For functional annotation, the final gene set for each species was analyzed using Pfam, PRINTS, PANTHER, SUPERFAMILY, SMART, and Gene 3D in InterProScan v5.39-77.0 (Jones et al. 2014).

The carbohydrate-active enzymes (CAZymes) were predicted by aligning all protein-coding genes in each species against the dbCAN2 database (Zhang et al. 2018) using DIAMOND v0.9.24.125, HMMER v3.0, and Hotpep. Those supported by more than two aligners were considered as CAZymes. The Secondary Metabolite Unknown Regions Finder (SMURF) was used to predict SM gene clusters (Khaldi et al. 2010). Secreted proteins were identified using multiple processes. SignalP v5.1 (Petersen et al. 2011) was initially used to predict the candidates. Subsequently, putative membrane proteins were filtered out using TMHMM v2.0 (Krogh et al. 2001). Likely mitochondrial or endoplasmic reticulum proteins were removed using WoLF PSORT, TargetP v2.0, and Deeploc v2.0 (de Castro et al. 2006; Horton et al. 2007; Armenteros et al. 2019).

Phylogenomic data matrix construction and analysis

Concatenation is a popular method for inferring organismal histories (Steenwyk et al. 2023) and has been successfully used to infer evolutionary relationships in fungi (Li et al. 2021). Orthologous relationships among the genes in 21 NTF and 21 non-NTF were determined using OrthoFinder v2.2.6, with default settings (Emms and Kelly 2019). Single-copy genes present in all species were used for phylogenetic analysis. For each group of single-copy orthologous genes, their predicted protein sequences were aligned using MAFFT v7.453 (Katoh and Standley 2013). Aligned sequences were trimmed using the “gappyout” model in trimAl v1.2 (Capella-Gutiérrez et al. 2009), which has been demonstrated to be an efficacious approach for trimming (Tan et al. 2015; Steenwyk et al. 2020c), and concatenated. A maximum likelihood tree was generated using RAxML v8.2.12 (Stamatakis 2014) under the Q.insect+F+I+R10 model, which was automatically selected, with a discrete gamma distribution of rates across sites. 1,000 bootstrap resamplings were performed to evaluate bipartition support.

Analysis of Pfam domains

To characterize the patterns of functional diversification in functional domains across the NTF genomes, the copy numbers of each Pfam domain in 21 NTF and 21 non-NTF were subjected to principal component analysis (PCA) using the "prcomp" function in the stat package of R v3.5.1 with default settings (R Core Team 2017). We ranked the contribution to the first principal component (PC1) in descending order and selected the top 10% to display via a heatmap using the Pheatmap v1.0.12 package of R. The number of Pfam domains for each species was normalized using zero-mean normalization, and the corresponding profiles were shown in the heatmap.

Statistical analysis

Enrichment analysis of Pfam domains in NTF-specific genes was tested by Mann-Whitney U test (McKnight and Najab 2010). The p-values were corrected using the Bonferroni method. Comparison of the number of CAZymes involved in cellulose degradation with or without carbohydrate-binding module (CBM) between NTF and non-NTF was carried out using Mann-Whitney U test utilizing "wilcox.test" function in the stat package of R. The results were visualized using the ggplot2 package v3.3.2 of R (Wickham 2009).

Transcriptome analysis

Published transcriptome data of *D. dactyloides* (Accession: PRJNA723922), which forms constricting rings, and *A. oligospora* (Accession: PRJNA791406), which forms adhesive nets, (Fan et al. 2021; Yang et al. 2022) were downloaded from GenBank, and transcriptome data of *Da. haptotyla*, which forms adhesive knobs, was generated by us (unpublished). Normalized read counts were used to estimate gene expression levels, and those expressed at low levels (read counts < 5) were removed. Expression levels of the genes predicted to be involved in the niche adaptation based on our comparative genome analysis were compared in the presence (24 hr) and absence (0 hr) of preys (*Caenorhabditis elegans*). Genes with padj < 0.05 and |log2 Foldchange| >1 were considered differentially expressed.

MurE disruption and nematode attraction assay

The *DdaMurE* gene in *D. dactyloides* strain 29 (CGMCC3.20198) was disrupted using a published protocol (Fan et al. 2021). To determine whether the mutation

affects nematode attraction, 6-mm diameter plugs (collected 0.5 cm away from the edge of plates) from 14-day-old PDA cultures of *D. dactyloides* strain 29 (WT) and three *ΔDdaMurE* mutants were placed on water agar medium, and 6-mm diameter plugs of PDA medium were used as controls. 200 nematodes were added to the central location (a circle with the radius of 0.5 cm), with 5 replicates for each sample. We employed the attractive index system described in a study by Le Saux and Queneherve (2002). The system records the degree of attraction or repulsion using numbers ranging from +2 (attraction) to -2 (repulsion). Attractive indexes were calculated 6 h after placing the plates under shade. The resulting numbers were analyzed using SPSS v20.0, and significant differences were determined by a p-value < 0.01 using Student's t-test.

Acknowledgments

We want to thank Prof. Antonis Rokas, Department of Biological Sciences at Vanderbilt University and Prof. Yafei Mao, College of Life Science, Shanghai Jiaotong University for providing valuable suggestions. This work was supported by the National Natural Science Foundation of China (grant numbers 32020103001 and 31770065) and the Startup Fund from the Nankai University to X. L. S. K. was supported by the USDA-NIFA and Federal Appropriations (Projects PEN4655 and PEN4839). J. L. S. is a Howard Hughes Medical Institute Awardee of the Life Sciences Research Foundation.

Author contributions

X. L., M. X. and Y. F. designed the research; Y. F., M. D., W. D., L.Y. and W. Z. performed the research; Y. F., E. Y., S. W., L. Z., M. X. and X. L. contributed new reagents/analytic tools; M. D., Y. F., W. Z. W. D. and E. Y. analyzed the data; E. Y., S. K., Z. A. and X. L supervised the data analysis; Y. F., E. Y., S. K., J. S., Z. A., M. D. and X. L. wrote the paper. All authors reviewed and approved the manuscript.

Competing interest

JLS is an advisor for ForensisGroup Inc. The authors have no relevant financial or non-financial interests to disclose.

Data availability

Data from the whole genome shotgun sequencing of 16 NTF reported in this paper are

available at GenBank under the BioProject number PRJNA791178 (https://www.ncbi.nlm.nih.gov/bioproject/791178). Corresponding accession numbers are JAJTUI000000000 (*Arthrobotrys conoides*), JAJTTS000000000 (*A. iridis*), JAJTTT000000000 (*A. musiformis*), JAJTTU000000000 (*A. pseudoclavata*), JAJTTV000000000 (*A. sinensis*), JAJTTW000000000 (*A. sphaeroides*), JAJTTX000000000 (*A. vermicola*), JAJTTY000000000 (*Dactylellina cionopaga*), JAJTUB000000000 (*D. drechsleri*), JAJTUC000000000 (*D. leptospora*), JAJTUD000000000 (*D. parvicollis*), JAJTUE000000000 (*D. querci*), JAKDFA000000000 (*D. tibetensis*), JAJTUF000000000 (*Drechslerella brochopaga*), JAJTUH000000000 (*Dr. coelobrocha*), and JAJTUG000000000 (*Dr. dactyloides*).

References

Andersson KM, Kumar D, Bentzer J, Friman E, Ahren D, Tunlid A. 2014. Interspecific and host-related gene expression patterns in nematode-trapping fungi. BMC Genomics 15:968.

Andersson KM, Meerupati T, Levander F, Friman E, Ahren D, Tunlid A. 2013. Proteome of the nematode-trapping cells of the fungus *Monacrosporium haptotylum*. Appl Environ Microb. 79:4993-5004.

Armenteros JJA, Salvatore M, Emanuelsson O, Winther O, von Heijne G, Elofsson A, Nielsen H. 2019. Detecting sequence signals in targeting peptides using deep learning. Life Sci Alliance 2:e201900429.

Bajic D, Sanchez A. 2020. The ecology and evolution of microbial metabolic strategies. Curr Opin Biotechnol. 62:123-128.

Barron GL. 1992. Lignolytic and cellulolytic fungi as predators and parasites. In: Carroll GC, Wicklow DT. (eds). The fungal Community: Its Organization and Role in the Ecosystem. Abingdon: Routledge. p. 311-326.

Barron GL. 2003. Predatory fungi, wood decay, and the carbon cycle. Biodiversity 4:3-9.

Barreteau H, Kovac A, Boniface A, Sova M, Gobec S, Blanot D. 2008. Cytoplasmic steps of peptidoglycan biosynthesis. FEMS Microbiol Rev 32(2):168-207.

Boetzer M, Henkel CV, Jansen HJ, Butler D, Pirovano W. 2011. Scaffolding pre-

assembled contigs using SSPACE. Bioinformatics 27:578-579.

Bolger AM, Lohse M, Usadel B. 2014. Trimmomatic: a flexible trimmer for Illumina sequence data. Bioinformatics 30:2114-2120.

Bugg TD, Braddick D, Dowson CG, Roper DI. 2011. Bacterial cell wall assembly: still an attractive antibacterial target. Trends Biotechnol 29(4):167-73.

Capella-Gutiérrez S, Silla-Martínez JM, Gabaldón T. 2009. trimAl: a tool for automated alignment trimming in large-scale phylogenetic analyses. Bioinformatics 25:1972-1973.

Chundawat S, Nemmaru B, Hackl M, Brady S, Hilton M, Johnson M, Chang S, Lang M, Hyun H, Lee S-H, et al. 2021. Molecular origins of reduced activity and binding commitment of processive cellulases and associated carbohydrate-binding proteins to cellulose III. J Biol Chem. 296:100431.

Darwiche R, Kelleher A, Hudspeth EM, Schneiter R, Asojo OA. 2016. Structural and functional characterization of the CAP domain of pathogen-related yeast 1 (Pry1) protein. Sci Rep. 6:28838.

de Castro E, Sigrist CJ, Gattiker A, Bulliard V, Langendijk-Genevaux PS, Gasteiger E, Bairoch A, Hulo N. 2006. ScanProsite: detection of PROSITE signature matches and ProRule-associated functional and structural residues in proteins. Nucleic Acids Res. 34:W362-W365.

de Ulzurrun GVD, Hsueh YP. 2018. Predator-prey interactions of nematode-trapping fungi and nematodes: both sides of the coin. Appl Microbiol Biotechnol. 102:3939-3949.

de Vries RP, Makela MR. 2020. Genomic and postgenomic diversity of fungal plant biomass degradation approaches. Trends Microbiol. 28:487-499.

Emms DM, Kelly S. 2019. OrthoFinder: phylogenetic orthology inference for comparative genomics. Genome Biol. 20:238.

Espagne E, Lespinet O, Malagnac F, Da Silva C, Jaillon O, Porcel BM, Couloux A, Aury JM, Segurens B, Poulain J, et al. 2008. The genome sequence of the model ascomycete fungus *Podospora anserina*. Genome Biol. 9:R77.

498 Ezcurra MD, Butler RJ. 2018. The rise of the ruling reptiles and ecosystem recovery
499 from the Permo-Triassic mass extinction. Proc R Soc B. 285:20180361.

500 Fan YN, Zhang WW, Chen Y, Xiang MC, Liu XZ. 2021. DdaSTE12 is involved in
501 trap formation, ring inflation, conidiation, and vegetative growth in the
502 nematode-trapping fungus *Drechslerella dactyloides.* Appl Microbiol Biotechnol.
503 105:7379-7393.

504 Feurtey A, Stukenbrock Eva H. 2018. Interspecific gene exchange as a driver of
505 adaptive evolution in fungi. Ann Rev Microbiol 72: 377-398.

506 Floudas D, Binder M, Riley R, Barry K, Blanchette RA, Henrissat B, Martínez AT et
507 al. The Paleozoic origin of enzymatic lignin decomposition reconstructed from
508 31 fungal genomes. *Science.* 2012:336(6089):1715-1719.

509 Gibbs GM, Roelants K, O'Bryan MK. 2008. The CAP superfamily: cysteine-rich
510 secretory proteins, antigen 5, and pathogenesis-related 1 proteins-roles in
511 reproduction, cancer, and immune defense. Endocr Rev. 29:865-897.

512 Gregoire, J.M., Zhou, L., Haber, J.A. 2023. Combinatorial synthesis for AI-driven
513 materials discovery. Nat Synth. 2:493-504.

514 Gnerre S, MacCallum I, Przybylski D, Ribeiro FJ, Burton JN, Walker BJ, Sharpe T,
515 Hall G, Shea TP, Sykes S, et al. 2011. High-quality draft assemblies of
516 mammalian genomes from massively parallel sequence data. Proc Natl Acad Sci
517 U S A. 108:1513-1518.

518 Gonçalves C, Gonçalves P. 2019. Multilayered horizontal operon transfers from
519 bacteria reconstruct a thiamine salvage pathway in yeasts. Proc Natl Acad Sci U
520 S A. 116(44):22219-22228.

521 Hittinger CT, Rokas A. 2019. Extensive loss of cell-cycle and DNA repair genes in an
522 ancient lineage of bipolar budding yeasts. PLoS Biol 17(5):e3000255.

523 Hoff KJ, Lange S, Lomsadze A, Borodovsky M, Stanke M. 2016. BRAKER1:
524 unsupervised RNA-seq-based genome annotation with GeneMark-ET and
525 AUGUSTUS. Bioinformatics 32:767-769.

526 Horton P, Park KJ, Obayashi T, Fujita N, Harada H, Adams-Collier CJ, Nakai K. 2007.

527 WoLF PSORT: protein localization predictor. Nucleic Acids Res. 35:W585-
528 W587.

529 Ji XL, Yu ZF, Yang JK, Xu JP, Zhang Y, Liu SQ, Zou CG, Li J, Liang LM, Zhang KQ.
530 2020. Expansion of adhesion genes drives pathogenic adaptation of nematode-
531 trapping fungi. iScience 23:101057.

532 Jones P, Binns D, Chang HY, Fraser M, Li W, McAnulla C, McWilliam H, Maslen J,
533 Mitchell A, Nuka G, et al. 2014. InterProScan 5: genome-scale protein function
534 classification. Bioinformatics 30:1236-1240.

535 Katoh K, Standley DM. 2013. MAFFT multiple sequence alignment software version
536 7: improvements in performance and usability. Mol Biol Evol. 30:772-780.

537 Keller NP. 2019. Fungal secondary metabolism: regulation, function and drug
538 discovery. Nat Rev Microbiol 17:167-180.

539 Khaldi N, Seifuddin FT, Turner G, Haft D, Nierman WC, Wolfe KH, Fedorova ND.
540 2010. SMURF: genomic mapping of fungal secondary metabolite clusters.
541 Fungal Genet Biol. 47:736-741.

542 Klosterman SJ, Subbarao KV, Kang SC, Veronese P, Gold SE, Thomma BPHJ, Chen
543 ZH, Henrissat B, Lee YH, Park J, et al. 2011. Comparative genomics yields
544 insights into niche adaptation of plant vascular wilt pathogens. PLoS Pathog.
545 7:e1002137.

546 Krogh A, Larsson B, von Heijne G, Sonnhammer EL. 2001. Predicting
547 transmembrane protein topology with a hidden Markov model: application to
548 complete genomes. J Mol Biol. 305:567-580.

549 Le Saux R, Queneherve P. 2002. Differential chemotactic responses of two plant-
550 parasitic nematodes, *Meloidogyne incognita* and *Rotylenchulus reniformis*, to
551 some inorganic ions. Nematology 4:99-105.

552 Lee CH, Chang HW, Yang CT, Wali N, Shie JJ, Hsueh YP. 2020. Sensory cilia as the
553 Achilles heel of nematodes when attacked by carnivorous mushrooms. Proc Natl
554 Acad Sci U S A. 117:6014-6022.

555 Li Y, Hyde KD, Jeewon R, Cai L, Vijaykrishna D, Zhang KQ. 2005. Phylogenetics

and evolution of nematode-trapping fungi (Orbiliales) estimated from nuclear and protein coding genes. Mycologia. 97:1034-1046.

Li Y, Steenwyk JL, Chang Y, Wang Y, James TY, Stajich JE, Spatafora JW, Groenewald M, Dunn CW, Hittinger CT, Shen XX, Rokas A. 2021. A genome-scale phylogeny of the kingdom Fungi. Cur Biol. 31(8):1653-1665.e5.

Liang LM, Shen RF, Mo YY, Yang JK, Ji XL, Zhang KQ. 2015. A proposed adhesin AoMad1 helps nematode-trapping fungus *Arthrobotrys oligospora* recognizing host signals for life-style switching. Fungal Genet Biol. 81:172-181.

Liu KK, Zhang WW, Lai YL, Xiang MC, Wang XN, Zhang XY, Liu XZ. 2014. *Drechslerella stenobrocha* genome illustrates the mechanism of constricting rings and the origin of nematode predation in fungi. BMC Genomics 15:114.

Lopez-Llorca LV, Maciá-Vicente JG, Jansson HB. 2007. Mode of action and interactions of nematophagous fungi. In: Ciancio A, Mukerji KG. (eds). Integrated Management and Biocontrol of Vegetable and Grain Crops Nematodes. Dordrecht: Springer. p. 43-59.

Lowery CM, Fraass AJ. 2019. Morphospace expansion paces taxonomic diversification after end Cretaceous mass extinction. Nat Ecol Evol. 3:900-904.

Marques DA, Jones FC, Di Palma F, Kingsley DM, Reimchen TE. 2018. Experimental evidence for rapid genomic adaptation to a new niche in an adaptive radiation. Nat Ecol Evol. 2:1128-1138.

Malar CM, Krüger M, Krüger C, Wang Y, Stajich JE, Keller J, Chen ECH, Yildirir G, Villeneuve-Laroche M, Roux C, Delaux PM, Corradi N. 2021. The genome of *Geosiphon pyriformis* reveals ancestral traits linked to the emergence of the arbuscular mycorrhizal symbiosis. Cur Biol. 31(7):1570-1577.e4.

Mays C, Vajda V, Frank TD, Fielding CR, Nicoll RS, Tevyaw AP, McLoughlin S. 2020. Refined Permian-Triassic floristic timeline reveals early collapse and delayed recovery of south polar terrestrial ecosystems. Geol Soc Am Bull. 132:1489-1513.

McKnight PE, Najab J. 2010. Mann-Whitney U Test. In: Weiner IB, Craighead WE, (eds). The Corsini Encyclopedia of Psychology. p. 1-1.

586 Meerupati T, Andersson KM, Friman E, Kumar D, Tunlid A, Ahren D. 2013. Genomic
587 mechanisms accounting for the adaptation to parasitism in nematode-trapping
588 fungi. PLoS Genet. 9:e1003909.

589 Milewski S, Gabriel I, Olchowy J. 2006. Enzymes of UDP-GlcNAc biosynthesis in
590 yeast. Yeast. 23(1):1-14.

591 Möller EM, Bahnweg G, Sandermann H, Geiger HH. 1992. A simple and efficient
592 protocol for isolation of high molecular weight DNA from filamentous fungi,
593 fruit bodies, and infected plant tissues. Nucleic Acids Res. 20:6115-6116.

594 Murat C, Payen T, Noel B, Kuo A, Morin E, Chen J, Kohler A, Krizsán K, Balestrini
595 R, Da Silva C, et al. 2018. Pezizomycetes genomes reveal the molecular basis of
596 ectomycorrhizal truffle lifestyle. Nat Ecol Evol, 2(12):1956-1965.

597 Nordbring-Hertz B, Jansson HB, Tunlid A. 2006. Nematophagous fungi. In:
598 Encyclopedia of Life Sciences. Chichester: John Wiley & Sons, Ltd. p. 1-11.

599 Nordbringhertz B, Stalhammarcarlemalm M. 1978. Capture of nematodes by
600 *Arthrobotrys oligospora*, an electron microscope study. Can J Bot -Rev Can Bot.
601 56:1297-1307.

602 Opulente DA, Leavitt LaBella A, Harrison MC, et al. Genomic and ecological factors
603 shaping specialism and generalism across an entire subphylum. Preprint. bioRxiv.
604 2023.06.19.545611.

605 Pace HC, Brenner C. 2001. The nitrilase superfamily: classification, structure and
606 function. Genome Biol. 2:1-9.

607 Patil, S.P., Dalal, K.S., Shirsath, L.P., Chaudhari, B.L. 2023. Microbial hyaluronidase:
608 its production, purification and applications. In: Verma P. (ed) Industrial
609 Microbiology and Biotechnology. Springer, Singapore.

610 Petersen TN, Brunak S, von Heijne G, Nielsen H. 2011. SignalP 4.0: discriminating
611 signal peptides from transmembrane regions. Nat Methods 8:785-786.

612 Pramer D. 1964. Nematode-trapping fungi. Science 144:382-388.

613 R Core Team. 2017. R: a language and environment for statistical computing. Vienna:
614 R Foundation for Statistical Computing.

615 Radkov AD, Hsu YP, Booher G, VanNieuwenhze MS. 2018. Imaging bacterial cell
616 wall biosynthesis. Annu Rev Biochem. 87:991-1014.

617 Raffa N, Keller NP. 2019. A call to arms: Mustering secondary metabolites for success
618 and survival of an opportunistic pathogen. PLoS Pathog 15(4), e1007606.

619 Rampino MR, Eshet-Alkalai Y, Koutavas A, Rodriguez S. 2020. End-Permian
620 stratigraphic timeline applied to the timing of marine and non-marine extinctions.
621 Palaeoworld 29:577-589.

622 Rankin CH. 2006. Nematode behavior: The taste of success, the smell of danger! Cur
623 Biol. 16(3): R89-R91.

624 Rohlfs M, Churchill ACL. Fungal secondary metabolites as modulators of interactions
625 with insects and other arthropods. Fungal Genet Biol 2011, 48(1):23-34.

626 Smith SD, Pennell MW, Dunn CW, Edwards SV. Phylogenetics is the New Genetics
627 (for Most of Biodiversity). *Trends Ecol Evol*. 2020:35(5):415-425.

628 Stamatakis A. 2014. RAxML version 8: a tool for phylogenetic analysis and post-
629 analysis of large phylogenies. Bioinformatics 30:1312-1313.

630 Steenwyk JL, Rokas A. 2017. Extensive copy number variation in fermentation-
631 related genes among *Saccharomyces cerevisiae* wine strains. G3 (Bethesda)
632 7(5):1475-1485.

633 Steenwyk JL, Mead ME, Knowles SL, Raja HA, Roberts CD, Bader O, Houbraken J,
634 Goldman GH, Oberlies NH, Rokas A. 2020a. Variation Among Biosynthetic
635 Gene Clusters, Secondary Metabolite Profiles, and Cards of Virulence Across
636 Aspergillus Species. Genetics 216(2), 481–497.

637 Steenwyk JL, Opulente DA, Kominek J, Shen XX, Zhou X, Labella AL, Bradley NP,
638 Eichman BF, Čadež N, Libkind D, DeVirgilio J, Hulfachor AB, Kurtzman CP,
639 Steenwyk JL, Lind AL, Ries LNA, Dos Reis TF, Silva LP, Almeida F, Bastos RW,
640 Fraga da Silva TFC, Bonato VLD, Pessoni AM, Rodrigues F, Raja HA, Knowles
641 SL, Oberlies NH, Lagrou K, Goldman GH, Rokas A. 2020b. Pathogenic
642 allodiploid hybrids of *Aspergillus* fungi. Cur Biol. 30(13):2495-2507.e7.

643 Steenwyk JL, Buida TJ III, Li Y, Shen X-X, Rokas A. 2020c. ClipKIT: A multiple

644 sequence alignment trimming software for accurate phylogenomic inference.
645 PLoS Biol 18(12): e3001007.

646 Steenwyk JL, Li Y, Zhou X, Shen XX, Rokas A. 2023. Incongruence in the
647 phylogenomics era. Nat Rev Genet. 24(12):834-850.

648 Tan G, Muffato M, Ledergerber C, Herrero J, Goldman N, Gil M, Dessimoz C. 2015.
649 Current Methods for Automated Filtering of Multiple Sequence Alignments
650 Frequently Worsen Single-Gene Phylogenetic Inference. Syst Biol 64(5):778-791.

651 Thomson N, Bentley S, Holden M, Parkhill J. 2003. Genome watch-fitting the niche
652 by genomic adaptation. Nat Rev Microbiol. 1:92-93.

653 Tunlid A, Jansson HB, Nordbringhertz B. 1992. Fungal attachment to nematodes.
654 Mycol Res. 96:401-412.

655 van den Hoogen J, Geisen S, Routh D, Ferris H, Traunspurger W, Wardle DA, de
656 Goede RGM, Adams BJ, Ahmad W, Andriuzzi WS, et al. 2019. Soil nematode
657 abundance and functional group composition at a global scale. Nature 572:194-
658 198.

659 Visscher H, Brinkhuis H, Dilcher DL, Elsik WC, Eshet Y, Looy CV, Rampino MR,
660 Traverse A. 1996. The terminal Paleozoic fungal event: evidence of terrestrial
661 ecosystem destabilization and collapse. Proc Natl Acad Sci U S A. 93:2155-2158.

662 Wang R, Wang J, Yang XY. 2015. The extracellular bioactive substances of
663 *Arthrobotrys oligospora* during the nematode-trapping process. Biol Control. 86:
664 60-65.

665 Wang SX & Liu XZ. 2023. Tools and basic procedures of gene manipulation in
666 nematode-trapping fungi. Mycology, 14(2): 75-90.

667 Wang X, Li GH, Zou CG, Ji XL, Liu T, Zhao PJ, Liang LM, Xu JP, An ZQ, Zheng X,
668 et al. 2014. Bacteria can mobilize nematode-trapping fungi to kill nematodes.
669 Nat. Commun. 5:5776.

670 Watkinson SC. 2016. Molecular ecology. In: Watkinson SC, Boddy L, Money NP,
671 (eds). The Fungi 3rd edition. Boston: Academic Press. p. 189-203.

672 Wickham H. 2009. ggplot2: Elegant Graphics for Data Analysis. New York: Springer.

673 Yang CT, Vidal-Diez de Ulzurrun G, Gonçalves A, Lin HC, Chang CW, Huang TY,
674 Chen SA, Lai CK, Tsai I, Schroeder F, et al. 2020. Natural diversity in the
675 predatory behavior facilitates the establishment of a robust model strain for
676 nematode-trapping fungi. Proc Natl Acad Sci U S A. 117:201919726.

677 Yang EC, Xu LL, Yang Y, Zhang XY, Xiang MC, Wang CS, An ZQ, Liu XZ. 2012.
678 Origin and evolution of carnivorism in the Ascomycota (fungi). Proc Natl Acad
679 Sci U S A. 109:10960-10965.

680 Yang L, Li XM, Bai N, Yang XW, Zhang KQ, Yang JK. 2022. Transcriptomic analysis
681 reveals that Rho GTPases regulate trap development and lifestyle transition of
682 the nematode-trapping fungus *Arthrobotrys oligospora*. Microbiol Spectr.
683 10:e0175921.

684 Yang XW, Ma N, Yang L, Zheng YQ, Zhen ZY, Li Q, Xie MH, Li J, Zhang KQ, Yang
685 JK. 2018. Two Rab GTPases play different roles in conidiation, trap formation,
686 stress resistance, and virulence in the nematode-trapping fungus *Arthrobotrys*
687 *oligospora*. Appl Microbiol Biotechnol. 102:4601-4613.

688 Yang Y, Yang EC, An ZQ, Liu XZ. 2007. Evolution of nematode-trapping cells of
689 predatory fungi of the Orbiliaceae based on evidence from rRNA-encoding DNA
690 and multiprotein sequences. Proc Natl Acad Sci U S A. 104:8379-8384.

691 Zhang H, Yohe T, Huang L, Entwistle S, Wu P, Yang Z, Busk PK, Xu Y, Yin Y. 2018.
692 dbCAN2: a meta server for automated carbohydrate-active enzyme annotation.
693 Nucleic Acids Res. 46:W95-W101.

694 Zhang W, Liu DD, Yu ZC, Hou B, Fan Y, Li ZH, Shang SJ, Qiao YD, Fu JT, Niu JK,
695 et al. 2020. Comparative genome and transcriptome analysis of the nematode-
696 trapping fungus *Duddingtonia flagrans* reveals high pathogenicity during
697 nematode infection. Biol Control. 143:104159.

698 Zhang WW, Chen J, Fan YN, Hussain M, Liu XZ, Xiang MC. 2021. The E3-ligase
699 AoUBR1 in N-end rule pathway is involved in the vegetative growth, secretome,
700 and trap formation in *Arthrobotrys oligospora*. Fungal Biol. 125(7).
701

Figures and Tables

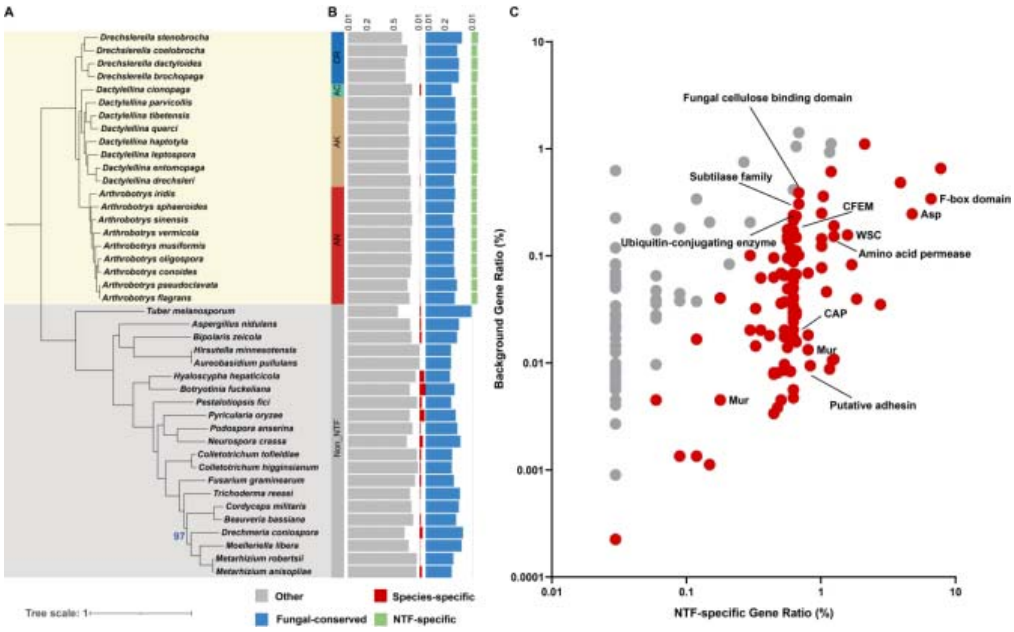

Fig. 1. Phylogenetic relationship of the species analyzed and characteristics of the genes in individual genomes. (A) Maximum likelihood phylogeny of 21 NTF (yellow background) and 21 non-NTF (gray background) constructed using protein sequences of 704 single-copy orthologous genes present in all species. The following color scheme was used to denote different trapping devices: green (adhesive columns, AC), gold (adhesive knobs, AK), red (adhesive nets, AN), and blue (constricting rings, CR). All bootstrap values were 100 unless otherwise indicated. (B) The bar chart shows the total number of protein-coding genes in each species. The genes were classified as fungal-conserved (blue), NTF-specific (green), species-specific (red), and those present only in some fungi (gray) based on OrthoFinder group. (C) The plot shows the distribution of Pfam domains among the NTF-specific genes. Each dot represented a gene illustrated by background gene ratio (%) and NTF-specific gene ratio (%) classified by Pfam domains. Enriched Pfam domains among the NTF-specific genes (see Dataset S1, Table S3) are highlighted in red (p-value < 0.05, Mann-Whitney U test) and include those associated with nematode capture (CFEM domain (PF05730)), nematode infection and consumption (eukaryotic aspartyl protease (PF00026), subtilase family (PF00082) and cysteine-rich secretory protein family (PF00188)), and ubiquitination degradation of proteins such as F-box domain (PF00646), amino acid permease (PF00324) and ubiquitin-conjugating enzyme

722 (PF00179).

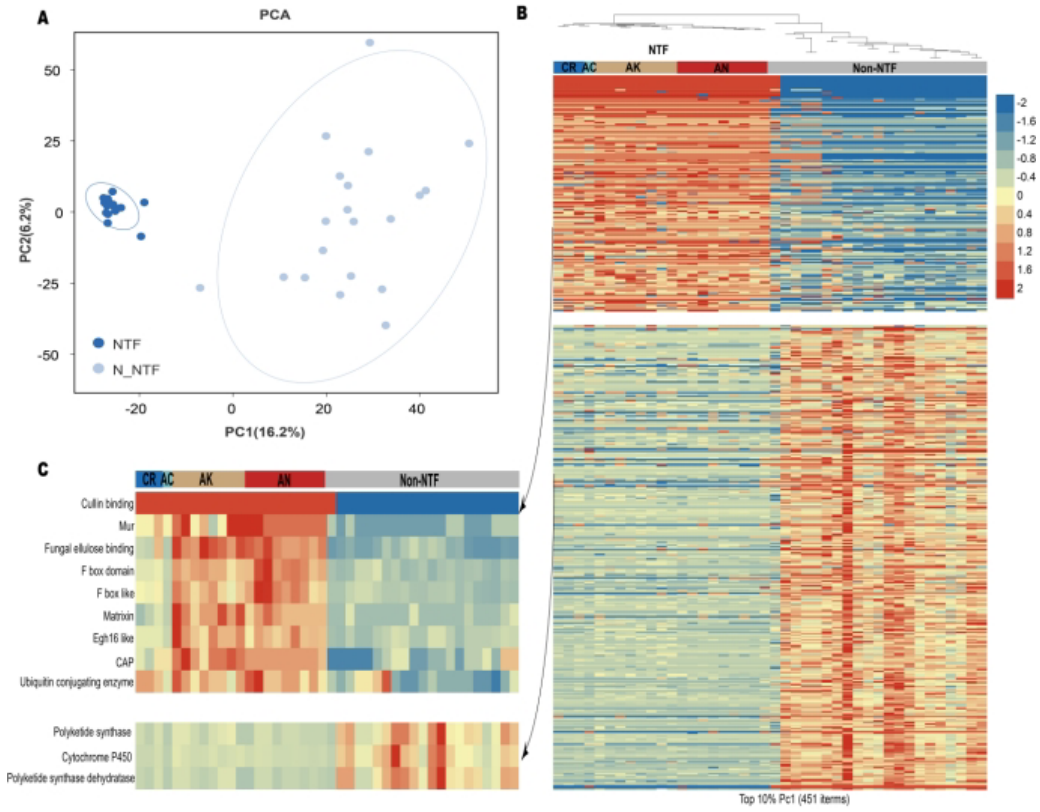

723 **Fig. 2. Contrasting diversification of protein domains between NTF and non-NTF.**
724 **(A)** Principal component analysis (PCA) based on the presence and number of Pfam
725 domains in multiple orthologous groups (OGs) across NTF and non-NTF. The first
726 two principal components account for 16.2% and 6.2% of variation, respectively. The
727 21 NTF are clustered together according to PC1. **(B)** Heatmaps were compiled from
728 the Pfam data that contributed most (top 10%, 451 items). Different patterns of Pfam
729 domain expansion and contraction are seen between NTF (yellow background) and
730 non-NTF (gray background) based on their normalized numbers. The following color
731 scheme was used to denote different trapping devices: green (adhesive columns, AC),
732 gold (adhesive knobs, AK), red (adhesive nets, AN), and blue (constricting rings, CR).
733 **(C)** Heatmaps highlighting the candidate Pfam domains related to carnivorous
734 lifestyle selected from those shown in **B**.
735

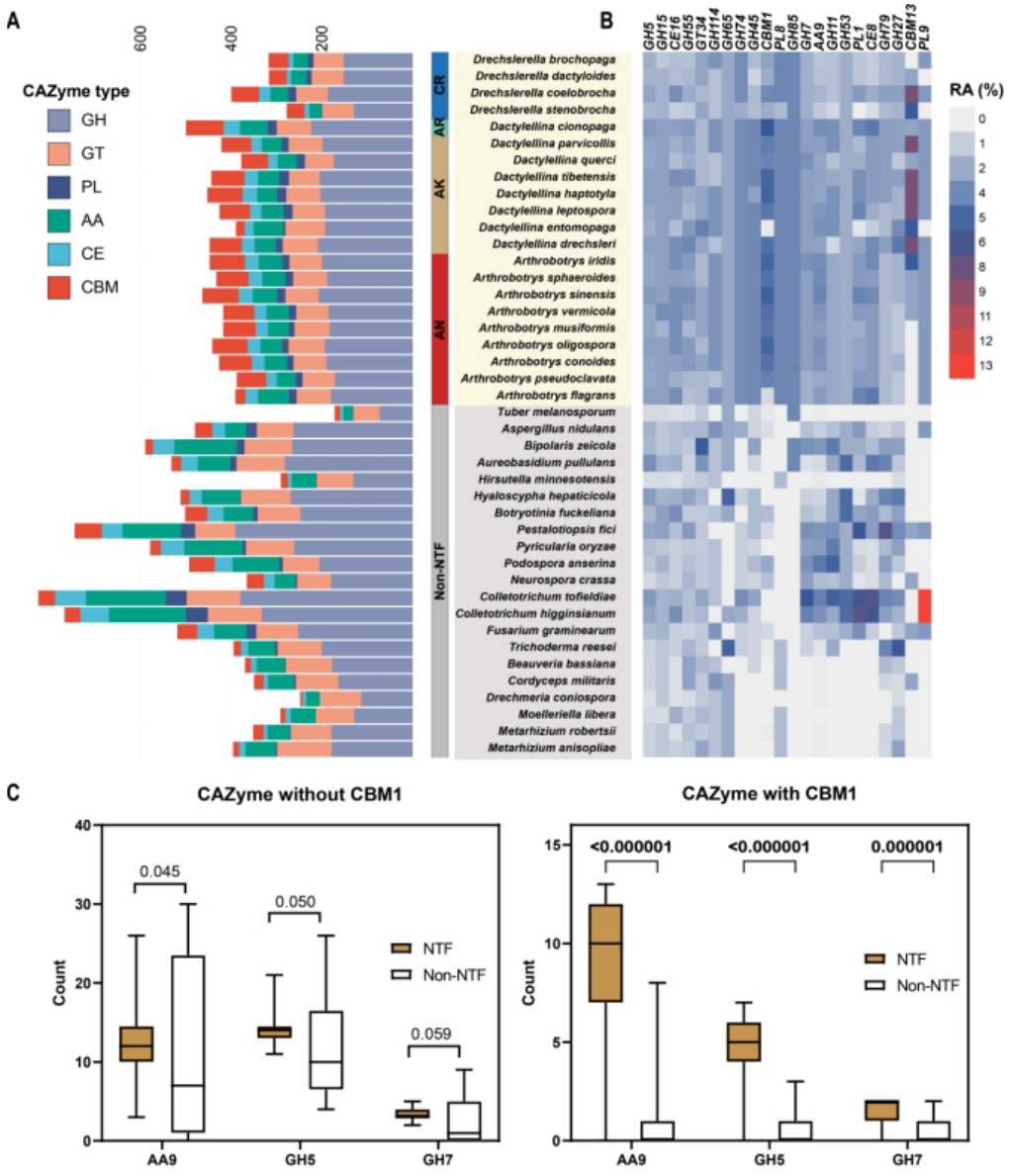

Fig. 3. Comparative analysis of the CAZymes among NTF and non-NTF. (**A**) The bar chart shows the numbers of the following CAZymes encoded by 21 NTF (yellow background) and 21 non-NTF (gray background): glycoside hydrolases (GH), glycosyl transferases (GT), carbohydrate esterases (CE), polysaccharide lyases (PL), auxiliary activities (AA), and carbohydrate-binding modules (CBM). The following color scheme was used to denote different trapping devices: green (adhesive columns, AC), gold (adhesive knobs, AK), red (adhesive nets, AN), and blue (constricting rings, CR). (**B**) Relative abundance (RA) profiles of 13 GHs, 2 GTs, 2 CBMs, 3 PLs, 1 AAs,

and 2 CEs involved in degrading cellulose. The gene number for each class was divided by the total gene number. (**C**) Comparison of the numbers of cellulose degrading enzymes with or without CBM1 between NTF (light brown) and non-NTF (white) using Mann-Whitney U test (*p*-values are shown on the graphs). The numbers of AA9, GH5, and GH7 without CBM1 (left) or with CBM1 (right) are presented.

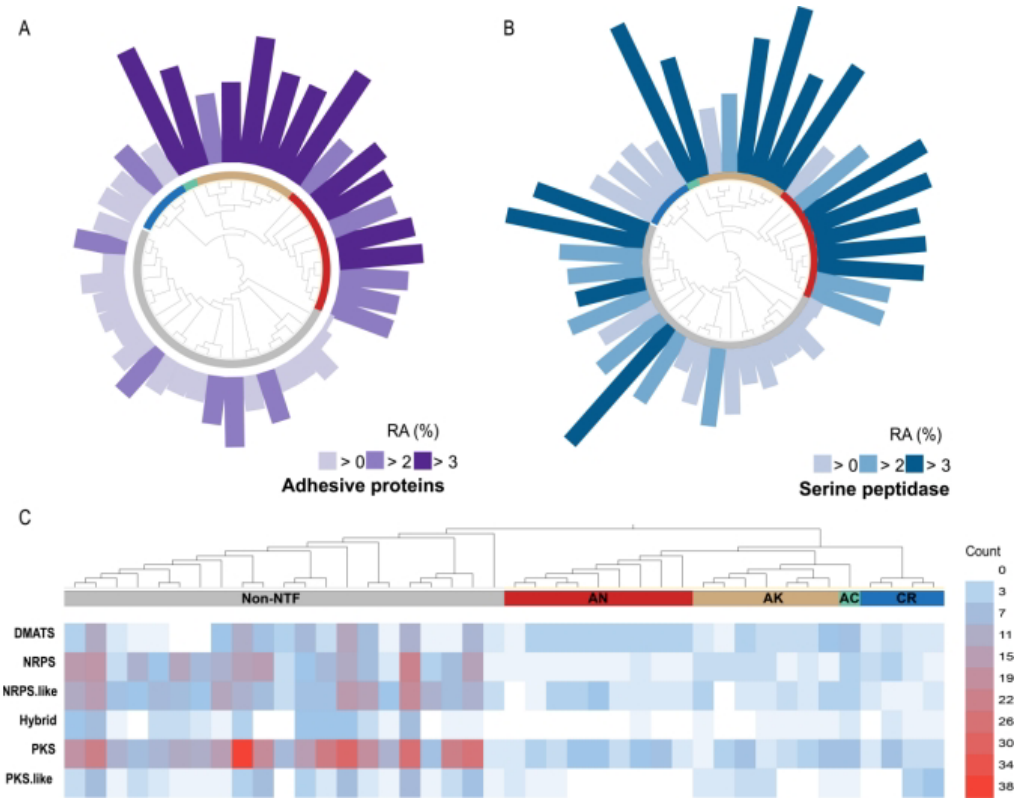

Fig. 4. Distribution patterns of adhesive proteins, serine peptidases, and secondary metabolism clusters among NTF and non-NTF. The following color schemes were used to denote different trapping devices: blue (constricting rings, CR), red (adhesive nets, AN), green (adhesive columns, AC), and gold (adhesive knobs, AK). (**A**, **B**) Relative abundance (RA) of adhesive proteins (**A**) and serine peptidases (**B**) among the total secreted proteins encoded by each species. The numbers of adhesive proteins and serine peptidases were divided by the total number of secreted proteins to calculate their RA. (**C**) A heatmap shows the numbers of different types of secondary metabolism gene clusters in each species.

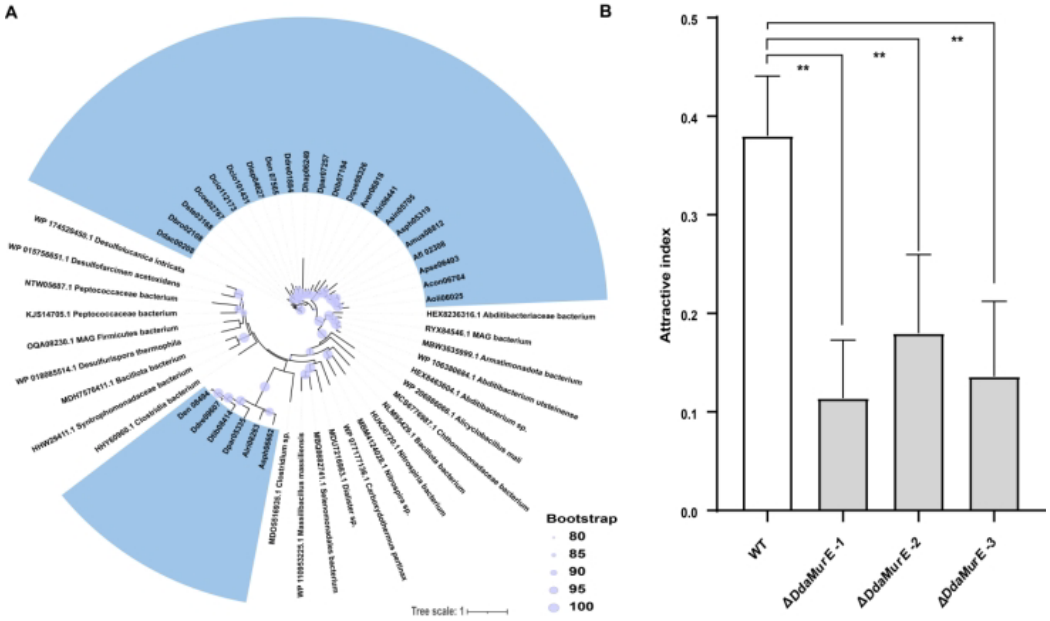

Fig. 5. The phylogenetic relationship and potential function of *MurE*. (A) Unrooted maximum-likelihood trees based on *MurE* protein sequences were constructed using RAxML. The bacterial species (only one genome sequence selected for each species) included were chosen based on the top 100 BlastP results with the corresponding *Arthrobotrys oligospora* protein sequences as queries. All NTF species included in blue background. (B) Attractive indexes of *Drechslerella dactyloides* wild type (WT) strain and three ΔDdaMurE mutants on water agar (WA) medium. ***p*-value < 0.01, two-tailed t-test, n = 5.

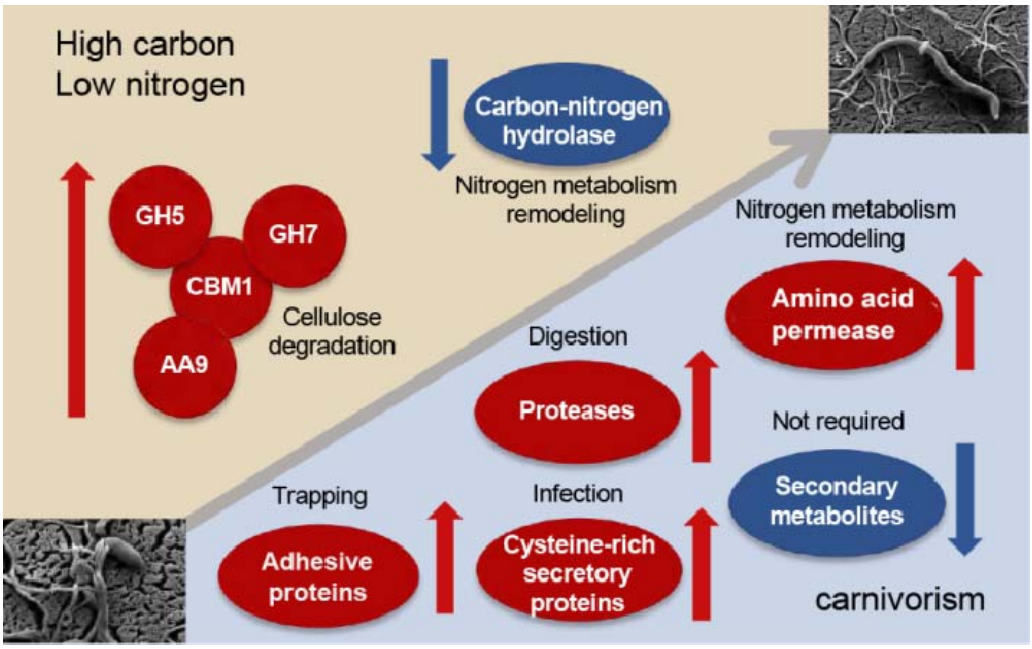

Fig. 6. Proposed model for genomic changes associated with the evolution of NTF. To adapt to carbon-rich/nitrogen-poor environments, the genes for aminotransferase class-III and cellulose degradation enzymes expanded, whereas the genes for carbon-nitrogen hydrolase contracted. The genes encoding adhesive proteins, cysteine-rich secretory proteins, and proteases, which are likely involved in nematode capture, infection, and consumption, respectively, were expanded to support carnivorism. The number of secondary metabolite gene clusters was significantly reduced.

777 **Table 1. Genome features of 21 nematode-trapping fungi**

Species[a]	Size (Mb)	N50 (Mb)	GC (%)	No. genes	Pfam (%)	BUSCO (%)
Arthrobotrys conoides	39.8	1.8	42.7	10,254	63.1	94.3
A. iridis	39.8	2.5	44.4	10,158	64.7	95.0
A. musiformis	40.8	2.0	44.3	10,510	63.0	95.1
A. oligospora	40.1	2.0	44.5	10,779	62.3	94.1
A. pseudoclavata	35.1	6.0	45.9	9,356	66.1	95.2
A. sinensis	40.6	2.3	45.6	11,240	62.1	95.5
A. sphaeroides	40.6	2.3	46.7	10,643	63.0	95.6
A. vermicola	40.7	1.6	45.6	10,501	63.0	95.7
A. flagrans	36.6	6.2	45	9927	68.2	93.4
Dactylellina cionopaga	47.4	2.1	43.8	12,524	61.5	93.8
Da. entomopaga	38.4	0.6	45	10470	61.0	94.6
Da. drechsleri	54.2	0.7	38.4	11,044	63.1	93.8
Da. haptotyla	38.9	0.2	45.7	10,353	65.1	94.5
Da. leptospora	36.9	1.2	44.6	9,986	65.4	94.5
Da. parvicollis	38.3	1.7	46.0	10,329	64.7	94.7
Da. querci	34.4	3.1	46.0	9,718	65.5	93.8
Da. tibetensis	36.4	1.9	45.1	10,165	65.6	93.7
Drechslerella brochopaga	35.8	1.9	50.5	9,044	67.1	96.1
Dr. coelobrocha	36.4	2.9	46.9	9,495	66.3	95.3
Dr. dactyloides	37.7	1.3	50.3	8,978	67.2	96.1
Dr. stenobrocha	30.2	4.8	50.4	7,955	70.0	94.5

778 [a]The sources of the sequenced strains and their accession numbers are shown in
779 Supplementary Table 1.